GBT POINTING EQUATIONS

J. J. CONDON

SUMMARY

Pointing errors will be a large or even dominant factor limiting the high-frequency performance of the GBT. The specified pointing error (about 1 arcsec rms) is so small and the GBT structure is so complex that there will likely be many significant causes of error. It is therefore important to make a mathematical model relating faults in the GBT structure (e.g., slightly tilted azimuth track) to the pointing data (astronomical measurements of calibrator positions, laser ranging measurements, etc.) that (1) is general enough to accommodate all possible pointing errors, anticipated and unanticipated, (2) helps to isolate and measure the different faults contributing to the measured pointing errors, (3) minimizes the corrected pointing residuals, and (4) is not too complicated for programmers to implement and observers to understand.

This memo outlines a method for modeling the GBT pointing. Rotation matrices and direction cosines are used to avoid the horrors of spherical trigonometry. Each small fault in the GBT is approximated by one or more infinitesimal rotations represented by an error matrix. Since these error matrices do not interact, their effects can be calculated independently and summed to give the total pointing error. All pointing errors are periodic functions of azimuth A and altitude a, so they can be written as two-dimensional Fourier series of trigonometric basis functions orthogonal in the region $-\pi \leq A \leq \pi$, $-\pi \leq a \leq \pi$. Most of the basis functions are also orthogonal in the region of sky accessible to the GBT ($-\pi \leq A \leq \pi$, $0 \leq a \leq \pi/2$). Thus the series coefficients are usually independent of each other. The traditional sources of error each require only one pointing term, and new terms may be added to model more complex pointing errors without disturbing the old values. Each Fourier series term automatically miminizes the rms pointing residual averaged over the sky. *The main recommendation of this memo is that the GBT pointing coefficients be drawn from the two-dimensional Fourier series coefficients whenever possible.*

As an example, this method was used to calculate the pointing errors resulting from irregularities in the height of the azimuth track. When applied to real pointing data from the 100 m telescope at Effelsberg, it revealed that track height variations with period π in azimuth significantly deform the alidade structure and twist the elevation axle about the vertical. Adding two pointing coefficients to the original 100 m telescope pointing model corrected for this effect and reduced the azimuthal pointing variance by 27%.

IDEAL ALT-AZ TELESCOPE GEOMETRY

The geometry of an ideal altitude-over-azimuth telescope mount is needed for all of the subsequent error analysis. In the "horizon" system of coordinates (x_h, y_h, z_h) centered on the observer, the reference plane is the horizon. The x_h axis points to the south point on the horizon, the y_h axis points to the east point on the horizon, and the z_h axis points to the "astronomical vertical" or zenith defined by a plumb line.

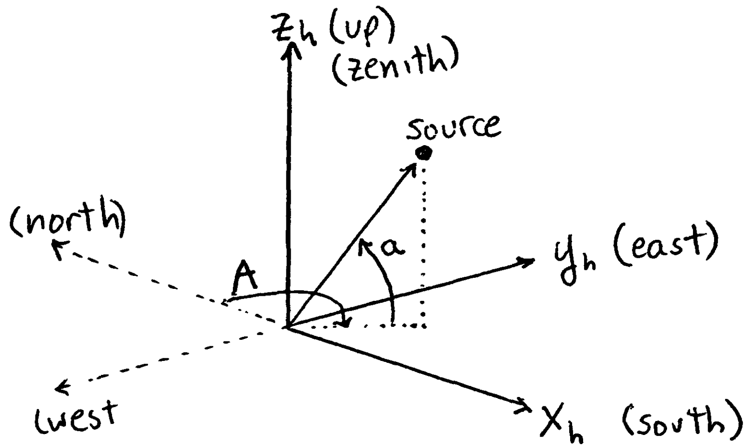

The altitude (sometimes called the elevation) a of a source is the angle from the horizon to the source measured along the great circle passing through the zenith. The azimuth A is conventionally measured from north through east by radio astronomers, as shown in the figure above. The unit vector H of direction cosines in the horizon system is therefore

$$H = \begin{pmatrix} x_h \\ y_h \\ z_h \end{pmatrix} = \begin{pmatrix} -\cos a \cos A \\ +\cos a \sin A \\ +\sin a \end{pmatrix} . \tag{1}$$

The ideal altitude-over-azimuth telescope mount has a rotating structure resting on the horizon plane that turns clockwise by the angle A about the $z_h = z_r$ axis when commanded to point at the source. The unit vector R in the rotated frame is obtained from H by a matrix multiplication (see Appendix for details). The direction cosines of the vector R are:

$$R = \begin{pmatrix} x_r \\ y_r \\ z_r \end{pmatrix} = \begin{pmatrix} +\cos(-A) & +\sin(-A) & 0 \\ -\sin(-A) & +\cos(-A) & 0 \\ 0 & 0 & 1 \end{pmatrix} \begin{pmatrix} x_h \\ y_h \\ z_h \end{pmatrix}$$

$$= \begin{pmatrix} +\cos A & -\sin A & 0 \\ +\sin A & +\cos A & 0 \\ 0 & 0 & 1 \end{pmatrix} \begin{pmatrix} -\cos a \cos A \\ +\cos a \sin A \\ +\sin a \end{pmatrix} = \begin{pmatrix} -\cos a \\ 0 \\ +\sin a \end{pmatrix} . \tag{2}$$

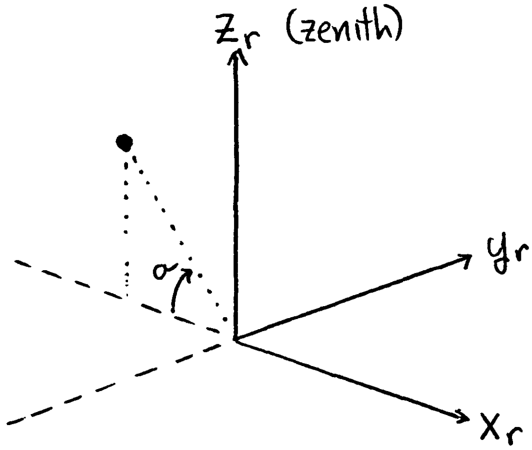

The ideal tipping structure mounted on the rotating structure tips the telescope clockwise by the angle $(\pi/2 - a)$ about the $y_r = y_t$ axis to point at the source.

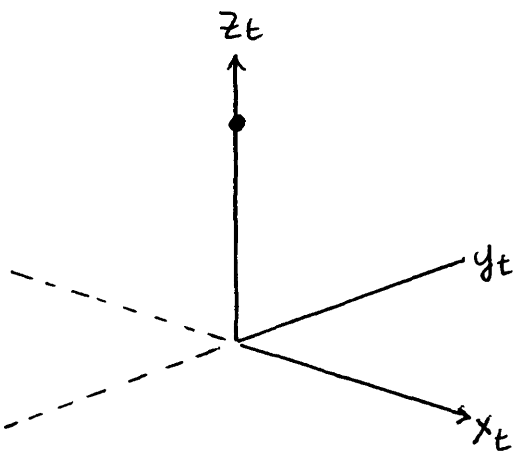

The unit vector T in the tipping frame becomes

$$T = \begin{pmatrix} x_t \\ y_t \\ z_t \end{pmatrix} = \begin{pmatrix} +\cos(a-\pi/2) & 0 & -\sin(a-\pi/2) \\ 0 & 1 & 0 \\ +\sin(a-\pi/2) & 0 & +\cos(a-\pi/2) \end{pmatrix} \begin{pmatrix} x_r \\ y_r \\ z_r \end{pmatrix}$$

$$= \begin{pmatrix} +\sin a & 0 & +\cos a \\ 0 & 1 & 0 \\ -\cos a & 0 & +\sin a \end{pmatrix} \begin{pmatrix} -\cos a \\ 0 \\ +\sin a \end{pmatrix} = \begin{pmatrix} 0 \\ 0 \\ 1 \end{pmatrix}, \tag{3}$$

and its direction cosines show that the z_t axis points to the source, as desired.

PROPAGATION OF SMALL POINTING ERRORS

The pointing errors produced by simple azimuth and altitude offsets in an imperfect telescope mount can be calculated directly from the rotation matrices for an ideal mount. Suppose the true azimuth of the rotating structure is A_r when the indicated azimuth is A. Then the azimuth error be defined as $\Delta A \equiv A_r - A$. Likewise, if the true altitude of the tipping structure is a_t when the indicated altitude is a, $\Delta a \equiv a_t - a$. The imperfect telescope mount will rotate to

$$R + \Delta R = \begin{pmatrix} +\cos A_r & -\sin A_r & 0 \\ +\sin A_r & +\cos A_r & 0 \\ 0 & 0 & 1 \end{pmatrix} \begin{pmatrix} -\cos a \cos A \\ +\cos a \sin A \\ +\sin a \end{pmatrix} = \begin{pmatrix} -\cos a \cos(A - A_r) \\ +\cos a \sin(A - A_r) \\ +\sin a \end{pmatrix}$$

and tip to

$$T + \Delta T = \begin{pmatrix} +\sin a_t & 0 & +\cos a_t \\ 0 & 1 & 0 \\ -\cos a_t & 0 & +\sin a_t \end{pmatrix} \begin{pmatrix} -\cos a \cos(A - A_r) \\ +\cos a \sin(A - A_r) \\ +\sin a \end{pmatrix} = \begin{pmatrix} -\sin \Delta a \\ -\cos a \sin \Delta A \\ +\cos \Delta a \end{pmatrix} .$$

If the mount errors ΔA, Δa are sufficiently small, error terms of order $(\Delta A)^2$, $(\Delta a)^2$ and higher may be neglected. How small is sufficiently small? Small enough that the approximation will not introduce errors comparable with the hoped-for GBT pointing accuracy, about 1 arcsec. This first-order approximation leaves errors of order $(\Delta A)^2$, $(\Delta a)^2$ rad, which should be < 1 arcsec $\approx 5 \times 10^{-6}$ rad so long as the mount errors are smaller than $\sqrt{5 \times 10^{-6}}$ rad ≈ 8 arcmin. All of the GBT mount errors should be much smaller than this. To first order in ϵ, $\sin \epsilon \approx \epsilon$ and $\cos \epsilon \approx 1$. Thus

$$T + \Delta T \approx \begin{pmatrix} -\Delta a \\ -\Delta A \cos a \\ 1 \end{pmatrix} = \begin{pmatrix} 0 \\ 0 \\ 1 \end{pmatrix} + \begin{pmatrix} -\Delta a \\ -\Delta A \cos a \\ 0 \end{pmatrix} . \qquad (4)$$

The components ΔT_x and ΔT_y are called the "vertical" and "horizontal" pointing errors, respectively. A "vertical" pointing correction $-\Delta T_x = +\Delta a$ and a "horizontal" pointing correction $-\Delta T_y = +\Delta A \cos a$ must be applied to cancel these pointing errors.

Most other mount errors, including deformations as well as rotations, can be described by introducing new reference frames that represent rotations about small angles. For example, suppose the rotating structure rests on an azimuth track that does not lie in the horizon plane, but whose normal is tilted by a small angle Δ_N to the north.

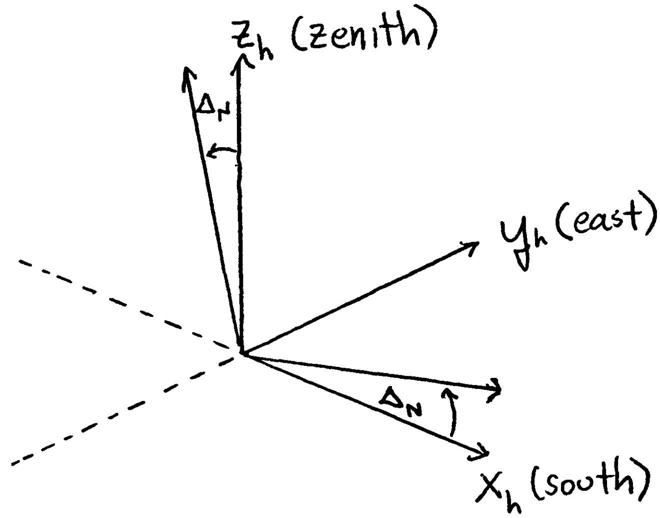

This small tilt is represented by the matrix for a clockwise rotation through the angle Δ_N about the y_h axis:

$$\begin{pmatrix} +\cos\Delta_N & 0 & +\sin\Delta_N \\ 0 & 1 & 0 \\ -\sin\Delta_N & 0 & +\cos\Delta_N \end{pmatrix} \approx \begin{pmatrix} 1 & 0 & +\Delta_N \\ 0 & 1 & 0 \\ -\Delta_N & 0 & 1 \end{pmatrix} .$$

Similarly, a small tilt Δ_W to the west is equivalent to a counterclockwise rotation by Δ_W about the x_h axis:

$$\begin{pmatrix} 1 & 0 & 0 \\ 0 & +\cos\Delta_W & +\sin\Delta_W \\ 0 & -\sin\Delta_W & +\cos\Delta_W \end{pmatrix} \approx \begin{pmatrix} 1 & 0 & 0 \\ 0 & 1 & +\Delta_W \\ 0 & -\Delta_W & 1 \end{pmatrix} .$$

To first order in Δ_N and Δ_W, these small tilt matrices commute, so an arbitrary small tilt of the azimuth track supporting the rotating structure can be represented by the unique product matrix

$$\begin{pmatrix} 1 & 0 & +\Delta_N \\ 0 & 1 & +\Delta_W \\ -\Delta_N & -\Delta_W & 1 \end{pmatrix} = \begin{pmatrix} 1 & 0 & 0 \\ 0 & 1 & 0 \\ 0 & 0 & 1 \end{pmatrix} + \begin{pmatrix} 0 & 0 & +\Delta_N \\ 0 & 0 & +\Delta_W \\ -\Delta_N & -\Delta_W & 0 \end{pmatrix} .$$

The unit vector H (Equation 1) pointing to the source in the horizon frame is transformed by the tilt matrix to the unit vector $H + \Delta H$ in the tilted frame:

$$H + \Delta H \approx \begin{pmatrix} x_h \\ y_h \\ z_h \end{pmatrix} + \begin{pmatrix} 0 & 0 & +\Delta_N \\ 0 & 0 & +\Delta_W \\ -\Delta_N & -\Delta_W & 0 \end{pmatrix} \begin{pmatrix} x_h \\ y_h \\ z_h \end{pmatrix} .$$

Apart from being tilted, the telescope mount is assumed to be perfect, so the vector $H+\Delta H$ is transformed by the ideal-telescope rotation matrices in Equations (2) and (3) to

$$R+\Delta R \approx \begin{pmatrix} -\cos a \\ 0 \\ +\sin a \end{pmatrix} + \begin{pmatrix} +\Delta_N \cos A \sin a - \Delta_W \sin A \sin a \\ +\Delta_N \sin A \sin a + \Delta_W \cos A \sin a \\ +\Delta_N \cos A \cos a - \Delta_W \sin A \cos a \end{pmatrix} ,$$

and finally to

$$T+\Delta T \approx \begin{pmatrix} 0 \\ 0 \\ 1 \end{pmatrix} + \Delta_N \begin{pmatrix} +\cos A \\ +\sin A \sin a \\ 0 \end{pmatrix} + \Delta_W \begin{pmatrix} -\sin A \\ +\cos A \sin a \\ 0 \end{pmatrix} ,$$

so

$$\Delta T \approx \begin{pmatrix} +\Delta_N \cos A - \Delta_W \sin A \\ +\Delta_N \sin A \sin a + \Delta_W \cos A \sin a \\ 0 \end{pmatrix} . \tag{5}$$

Thus tilting the azimuth track by the small angles Δ_N to the north and Δ_W to the west causes a "horizontal" pointing error ($\Delta_N \sin A \sin a + \Delta_W \cos A \sin a$) and a "vertical" pointing error ($\Delta_N \cos A - \Delta_W \sin A$).

Note that the effects of multiple small mount faults propagate directly through the appropriate rotation matrices for an ideal mount because multiplying any two first-order error matrices yields only negligible second-order terms. Consequently the pointing errors resulting from separate faults can be calculated independently and later added to yield the total pointing errors. Suppose, for example, that in addition to the small track tilts described above, the tipping axis is tilted by a small angle Δ_L counterclockwise about the x_r axis.

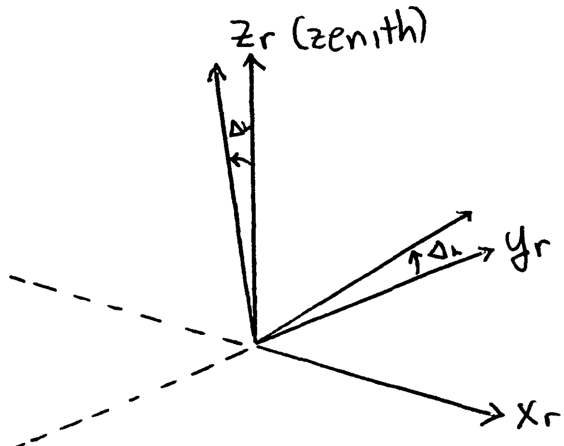

The tilt matrix describing such a mount collimation error is

$$\begin{pmatrix} 1 & 0 & 0 \\ 0 & +\cos\Delta_L & +\sin\Delta_L \\ 0 & -\sin\Delta_L & +\cos\Delta_L \end{pmatrix} \approx \begin{pmatrix} 1 & 0 & 0 \\ 0 & 1 & 0 \\ 0 & 0 & 1 \end{pmatrix} + \begin{pmatrix} 0 & 0 & 0 \\ 0 & 0 & +\Delta_L \\ 0 & -\Delta_L & 0 \end{pmatrix} .$$

The unit vector H (Equation 1) in the horizon frame is transformed to R in the ideal rotating frame by Equation (2). Then the mount collimation error matrix gives

$$\Delta R \approx \begin{pmatrix} 0 & 0 & 0 \\ 0 & 0 & +\Delta_L \\ 0 & -\Delta_L & 0 \end{pmatrix} \begin{pmatrix} -\cos a \\ 0 \\ +\sin a \end{pmatrix} = \begin{pmatrix} 0 \\ +\Delta_L \sin a \\ 0 \end{pmatrix}$$

and the ideal tipping matrix (Equation 3) yields the pointing error

$$\Delta T \approx \begin{pmatrix} +\sin a & 0 & +\cos a \\ 0 & 1 & 0 \\ -\cos a & 0 & +\sin a \end{pmatrix} \begin{pmatrix} 0 \\ +\Delta_L \sin a \\ 0 \end{pmatrix} = \begin{pmatrix} 0 \\ +\Delta_L \sin a \\ 0 \end{pmatrix} . \tag{6}$$

The total pointing error for a telescope with both azimuth track tilt and mount collimation errors is just the sum of the errors given individually by Equations (5) and (6).

Additional pointing errors can result from faults in the telescope itself. For example, horizontal and vertical telescope collimation errors directly cause horizontal and vertical pointing errors of the same size. Bending of the feed-support arm by the component of gravity perpendicular to the arm produces a vertical pointing error proportional to $\cos a$.

Traditional pointing analyses (e.g., Schraml, J. 1969, in "NRAO Miscellaneous Internal Reports 1966-1974" for the 36-foot telescope; Pauliny-Toth & Altenhoff 1972, Technischer Bericht Nr. 12, MPIfR, Bonn for the Effelsberg 100 m telescope; Ulich, B. L. 1976, NRAO Engineering Division Internal Report No. 105 for the 36-foot telescope; Ulich, B. L. 1981, Int. J. Infrared & Millimeter Waves, 2, 293) are based on a spherical trigonometric derivation (Stumpff, P. 1972, Kleinheubacher Berichte, 15, 431) of the terms derived above. The resulting horizontal and vertical pointing corrections have the form:

$$\Delta A \cos a \approx C_1 + C_2 \cos a + C_3 \sin a + C_4 \cos A \sin a + C_5 \sin A \sin a \ ,$$

where C_1 is adjusted to correct for a horizontal telescope collimation error, C_2 for a constant azimuth offset (Equation 4), C_3 for the tipping-mount collimation error (Equation 6), C_4 and C_5 correct for azimuth track tilt (Equation 5), and

$$\Delta a \approx C_6 + C_7 \cos a + C_4 \sin A + C_5 \cos A \ ,$$

where C_6 corrects for the vertical telescope collimation error and C_7 for gravitational bending. The coefficients C_n are found simultaneously by a least-squares fit to the measured pointing residuals, so changes in one affect the others. Depending on the range of altitude and azimuth covered by the data and on the pointing terms included, the solutions may be numerically unstable and wildly differing values of the pointing constants obtained from only slightly differing data sets (Condon, J. 1986, NRAO Electronics Division Technical Note No. 137). Also, the real causes of pointing errors are more complicated — the azimuth track may be irregular as well as tilted, for example. It will probably be necessary to correct for these complications to achieve 1 arcsec pointing accuracy. A method for doing this is outlined in the next section and applied in the last section of the memo.

A TWO-DIMENSIONAL FOURIER-SERIES REPRESENTATION

The horizontal and vertical components of the pointing error are each periodic functions of A and a, with period 2π in both coordinates. Any such periodic function $f(A, a)$ can be represented exactly by the two-dimensional Fourier series

$$
\begin{aligned}
f(A, a) = \sum_{q=0}^{\infty} \sum_{p=0}^{\infty} \big(& a_{p,q} \sin pA \sin qa + b_{p,q} \cos pA \sin qa \\
& + c_{p,q} \sin pA \cos qa + d_{p,q} \cos pA \cos qa \big) \ .
\end{aligned}
\tag{7}
$$

The series coefficients are

$$
\begin{aligned}
a_{p,q} &= \frac{(f, \sin pA \sin qa)}{\| \sin pA \sin qa \|^2} \ , \quad b_{p,q} = \frac{(f, \cos pA \sin qa)}{\| \cos pA \sin qa \|^2} \ , \\
c_{p,q} &= \frac{(f, \sin pA \cos qa)}{\| \sin pA \cos qa \|^2} \ , \quad d_{p,q} = \frac{(f, \cos pA \cos qa)}{\| \cos pA \cos qa \|^2} \ ,
\end{aligned}
\tag{8}
$$

where

$$
(f, g) \equiv \int \int_R f(A, a) g(A, a) dA da
$$

is the inner product of the functions f and g over the rectangular region R bounded by $-\pi \leq A \leq \pi$, $-\pi \leq a \leq \pi$ and $\|f\| \equiv (f, f)^{1/2}$ is the norm of f.

The price for modeling arbitrary pointing errors would seem to be an infinite number of pointing coefficients, but this need not be the case for two reasons: (1) Each of the traditional pointing terms described in the preceding section corresponds to a single low-order term in the expansion

$$
\begin{aligned}
f(A, a) = {} & d_{0,0} + c_{1,0} \sin A + d_{1,0} \cos A + b_{0,1} \sin a + d_{0,1} \cos a \\
& + a_{1,1} \sin A \sin a + b_{1,1} \cos A \sin a + c_{1,1} \sin A \cos a + d_{1,1} \cos A \cos a \\
& + c_{2,0} \sin 2A + d_{2,0} \cos 2A + b_{0,2} \sin 2a + d_{0,2} \cos 2a \\
& + a_{2,1} \sin 2A \sin a + b_{2,1} \cos 2A \sin a + c_{2,1} \sin 2A \cos a + d_{2,1} \cos 2A \cos a \\
& + \ldots
\end{aligned}
\tag{9}
$$

[$C_1 = d_{0,0}$, $C_2 = d_{0,1}$, $C_3 = b_{0,1}$, $C_4 = b_{1,1}$, $C_5 = a_{1,1}$ (horizontal error) and $C_4 = c_{1,0}$, $C_5 = d_{1,0}$, $C_6 = d_{0,0}$, $C_7 = d_{0,1}$ (vertical error)]. This Fourier series is therefore very efficient at representing the principal pointing terms, and each term of the series can be traced back to a particular fault in the telescope or its mount. (2) The basis functions are orthogonal over the region $-\pi \leq A \leq \pi$, $-\pi \leq a \leq \pi$, so the coefficients are independent. They may determined one at a time rather than simultaneously, and the error in determining one coefficient does not affect the values of other coefficients. Pointing coefficients determined from independent data sets should agree within the measurement errors, so that calibration data sets may be combined to reduce the errors or compared to check for changes in the pointing. Significant terms can be added and insignificant ones deleted at will. Most of the series terms will be insignificant and their coefficients can be set to zero. The coefficient (Equation 8) of each term minimizes the norm of the pointing residuals remaining after the partial series has been subtracted.

Unfortunately, the GBT cannot observe pointing calibrators over the full altitude range $-\pi \leq a \leq \pi$. The actual region R covered by the GBT is approximately $\pi \leq A \leq \pi$, $0 \leq a \leq \pi/2$. The basis functions above are not all orthogonal in this restricted region, so the measured values of some series coefficients will be correlated. If measurements are made uniformly over the region covered by the GBT, the coefficients for any pair of basis functions f and g will have a correlation coefficient (projection coefficient)

$$\chi(f,g) \equiv \frac{(f,g)}{\|f\|\|g\|} = \chi(g,f)\ . \tag{10}$$

Table 1 lists a number of these correlation coefficients, showing which must be determined simultaneously and which may be found independently. Careful selection of pointing terms made with the help of Table 1 can minimize the number of correlations. For example, the coefficient $c_{2,1}$ (needed for horizontal pointing errors caused by height irregularities in the azimuth ring — see the next section) is correlated with $c_{2,0}$ and $a_{2,1}$. But $c_{2,0}$ and $a_{2,1}$ are probably not needed and can be set to zero, so $c_{2,1}$ may be determined independently.

A PARTICULAR EXAMPLE: POINTING ERRORS CAUSED BY AN IRREGULAR AZIMUTH TRACK

In the horizon plane the azimuth track is a circle of radius ρ whose height η may vary irregularly with track azimuth ξ as shown below.

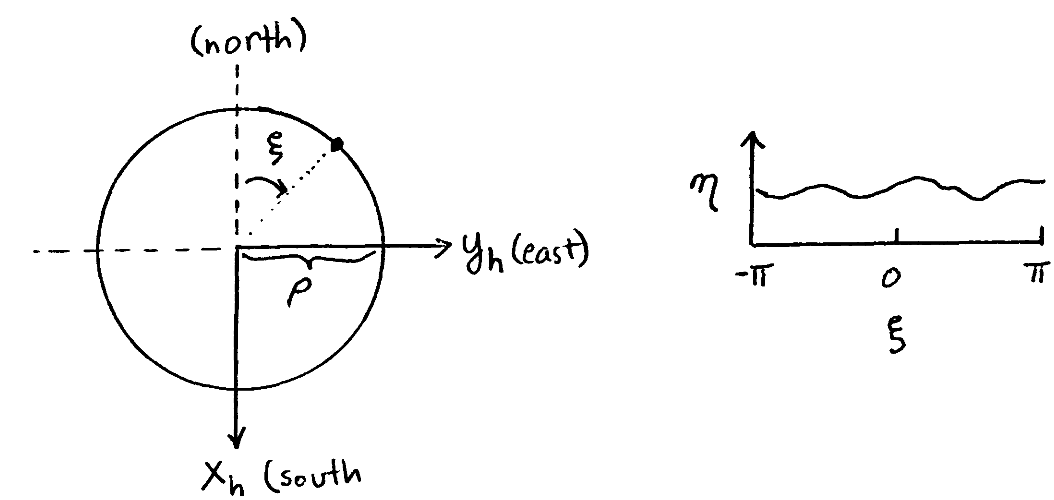

The only restrictions on $\eta(\xi)$ are that it be periodic over $-\pi \leq \xi \leq \pi$ and that $\eta/\rho \ll 1$.

The GBT rotating structure (alidade) is supported by four wheel trucks at ring azimuths $\xi_1 = A+\pi/4$, $\xi_2 = A+3\pi/4$, $\xi_3 = A+5\pi/4$, and $\xi_4 = A+7\pi/4$ when the alidade is rotated to azimuth A. This structure sags under the weight of the telescope, so all four wheels always rest on the track, even though the track is slightly irregular. The wheel heights above the horizon plane are thus $\eta_1 = \eta(A+\pi/4)$, $\eta_2 = \eta(A+3\pi/4)$, $\eta_3 = \eta(A+5\pi/4)$, and $\eta_4 = \eta(A+7\pi/4)$. A small height difference between opposing wheels 1 and 3 will tilt the alidade about the x_h and y_h axes by angles

$$\Delta_X \approx \left(\frac{\eta_3 - \eta_1}{2\rho}\right)\cos(\pi/4) \quad \text{and} \quad \Delta_Y \approx \left(\frac{\eta_1 - \eta_3}{2\rho}\right)\cos(\pi/4) \ ,$$

respectively. Similarly, the height difference between wheels 2 and 4 yields small tilts

$$\Delta_X \approx \left(\frac{\eta_2 - \eta_4}{2\rho}\right)\cos(\pi/4) \quad \text{and} \quad \Delta_Y \approx \left(\frac{\eta_2 - \eta_4}{2\rho}\right)\cos(\pi/4) \ .$$

Summing the effects of both wheel pairs yields

$$\Delta_X \approx \frac{\eta_2 + \eta_3 - \eta_1 - \eta_4}{2\sqrt{2}\rho} \quad \text{and} \quad \Delta_Y \approx \frac{\eta_1 + \eta_2 - \eta_3 - \eta_4}{2\sqrt{2}\rho} \ . \tag{11}$$

The figure below shows how stresses deform the alidade to rotate the elevation-axle about the z-axis as well.

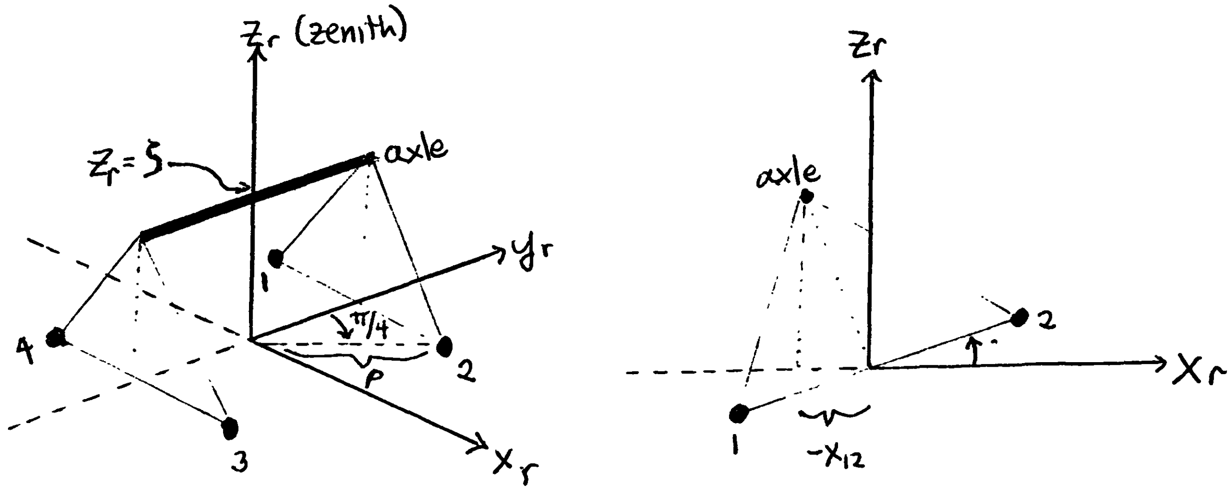

If the axle is at a height ζ above the track, the end supported by wheels 1 and 2 will be at x coordinate x_{12} and the other end at x_{34} given by

$$x_{12} \approx -\zeta\left[\frac{\eta_2 - \eta_1}{2\rho\cos(\pi/4)}\right] \quad \text{and} \quad x_{34} \approx -\zeta\left[\frac{\eta_3 - \eta_4}{2\rho\cos(\pi/4)}\right] \ .$$

This internal twisting of the alidade rotates the axle about the vertical by

$$\Delta_Z \approx \left(\frac{\zeta}{2\rho^2}\right)[(\eta_2 + \eta_4) - (\eta_1 + \eta_3)] \ . \tag{12}$$

Since small error matrices commute, all three error components can be compressed into a single error matrix. As in the derivation of Equation (5),

$$\Delta R \approx \begin{pmatrix} 0 & +\Delta_Z & +\Delta_X \\ -\Delta_Z & 0 & +\Delta_Y \\ -\Delta_X & -\Delta_Y & 0 \end{pmatrix} \begin{pmatrix} -\cos a \\ 0 \\ +\sin a \end{pmatrix} = \begin{pmatrix} +\Delta_X \sin a \\ +\Delta_Y \sin a + \Delta_Z \cos a \\ +\Delta_X \cos a \end{pmatrix} .$$

Transforming with the ideal tipping matrix (Equation 3) gives the pointing error

$$\Delta T \approx \begin{pmatrix} +\Delta_X \\ +\Delta_Y \sin a + \Delta_Z \cos a \\ 0 \end{pmatrix} . \tag{13}$$

The angles Δ_X, Δ_Y, and Δ_Z can be derived by inserting the Fourier series describing the track height

$$\eta(\xi) = b_0 + \sum_{n=1}^{\infty} (a_n \sin n\xi + b_n \cos n\xi)$$

into Equations (11) and (12). The results are

$$\begin{aligned} \rho\Delta_X \approx &- a_1 \sin A - b_1 \cos A + a_3 \sin 3A + b_3 \cos 3A \\ &+ a_5 \sin 5A + b_5 \cos 5A - a_7 \sin 7A - b_7 \cos 7A + \ldots \\ \rho\Delta_Y \approx &+ a_1 \cos A - b_1 \sin A + a_3 \cos 3A - b_3 \sin 3A \\ &- a_5 \cos 5A + b_5 \sin 5A - a_7 \cos 7A + b_7 \sin 7A + \ldots \\ \frac{\rho^2 \Delta_Z}{2\zeta} \approx &- a_2 \cos 2A + b_2 \sin 2A \\ &+ a_6 \cos 6A - b_6 \sin 6A + \ldots , \end{aligned}$$

where the sign patterns repeat every two lines. Entering these results into Equation (13) gives the pointing errors for the irregular azimuth track $\Delta T \approx$

$$\frac{1}{\rho} \begin{pmatrix} -a_1 \sin A - b_1 \cos A + a_3 \sin 3A + b_3 \cos 3A + \ldots \\ +a_1 \cos A \sin a - b_1 \sin A \sin a - (2a_2\zeta/\rho) \cos 2A \cos a + (2b_2\zeta/\rho) \sin 2A \cos a + \ldots \\ 0 \end{pmatrix} \tag{14}$$

The terms containing the angle A in Equation (14) measure the tilt of the track, just as Equation (5) does. The terms containing the angle $2A$ give pointing errors caused by twisting the elevation axle and are not included in the traditional pointing equations. However, their coefficients are twice those of the tilting terms for $\zeta \sim \rho$, so they may well be important. Thus at least $c_{2,1} \approx +2b_2\zeta/\rho^2$ and $d_{2,1} \approx -2a_2\zeta/\rho^2$ should be added to the pointing equations.

To see how large these terms might be in a real telescope, I used the Effelsberg 100 m telescope horizontal pointing residuals after the traditional pointing corrections had been made (Table 2), as reported by Pauliny-Toth & Altenhoff (1972, Technischer Bericht Nr. 12, MPIfR, Bonn). Table 1 shows that the Fourier coefficients $c_{2,1}$ and $d_{2,1}$ are independent of each other and of all others used in the 100 m telescope pointing corrections, so they can be calculated directly from the measured pointing residuals $f(A,a)$ listed in Table 2. The expressions

$$c_{2,1} = \frac{(f, \sin 2A \cos a)}{\|\sin 2A \cos a\|^2}, \quad d_{2,1} = \frac{(f, \cos 2A \cos a)}{\|\cos 2A \cos a\|^2}$$

were approximated by sums over the $N = 180$ data points $f_n(A,a)$:

$$c_{2,1} \approx \frac{\sum_{n=1}^{N} f_n \sin 2A \cos a}{\sum_{n=1}^{N} (\sin 2A \cos a)^2}, \quad d_{2,1} \approx \frac{\sum_{n=1}^{N} f_n \cos 2A \cos a}{\sum_{n=1}^{N} (\cos 2A \cos a)^2}.$$

The data in Table 2 yield $c_{2,1} \approx -3.2$ arcsec and $d_{2,1} \approx -2.0$ arcsec. This is equivalent to a horizontal pointing error $\approx 3.8 \cos[2(A - 120°)] \cos a$ arcsec. Its amplitude is comparable with the initial horizontal pointing residual (3.66 arcsec rms), and subtracting it reduces the rms residual to 3.11 arcsec. Thus the twisting term is quite significant in the 100 m telescope, and removing it reduces the horizontal pointing variance by 27%. It is likely to be important for the GBT, whose pointing accuracy should be much better.

APPENDIX: ROTATION MATRICES

If the two-dimensional cartesian coordinate system (x_1, y_1) is rotated counterclockwise by an angle α to yield the new system (x_2, y_2),

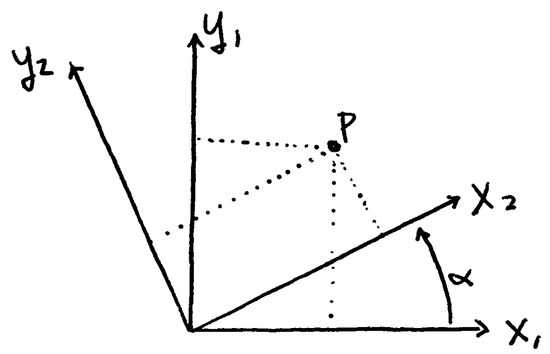

the coordinates of any point P are related by

$$
\begin{aligned}
x_2 &= y_2 \tan\alpha + x_1 / \cos\alpha \\
y_1 &= x_1 \tan\alpha + y_2 / \cos\alpha
\end{aligned}
$$

so

$$
\begin{aligned}
x_2 &= y_1 \sin\alpha + x_1 \cos\alpha \\
y_2 &= y_1 \cos\alpha - x_1 \sin\alpha \ .
\end{aligned}
$$

In matrix notation,

$$
\begin{pmatrix} x_2 \\ y_2 \end{pmatrix} = \begin{pmatrix} +\cos\alpha & +\sin\alpha \\ -\sin\alpha & +\cos\alpha \end{pmatrix} \begin{pmatrix} x_1 \\ y_1 \end{pmatrix} \ .
$$

For three-dimensional right-handed cartesian coordinate systems, the rotation matrices $R_x(\alpha)$, $R_y(\alpha)$, and $R_z(\alpha)$ describing counterclockwise rotations about the x, y, and z axes, respectively, are:

$$
R_x(\alpha) = \begin{pmatrix} 1 & 0 & 0 \\ 0 & +\cos\alpha & +\sin\alpha \\ 0 & -\sin\alpha & +\cos\alpha \end{pmatrix} \ ,
$$

$$
R_y(\alpha) = \begin{pmatrix} +\cos\alpha & 0 & -\sin\alpha \\ 0 & 1 & 0 \\ +\sin\alpha & 0 & +\cos\alpha \end{pmatrix} \ ,
$$

$$
R_z(\alpha) = \begin{pmatrix} +\cos\alpha & +\sin\alpha & 0 \\ -\sin\alpha & +\cos\alpha & 0 \\ 0 & 0 & 1 \end{pmatrix} \ .
$$

TABLE 1. Correlation coefficients $\chi(f,g)$ for the region $-\pi \leq A \leq \pi$, $0 \leq a \leq \pi/2$.

	$d_{0,0}$	$c_{1,0}$	$d_{1,0}$	$b_{0,1}$	$d_{0,1}$	$a_{1,1}$	$b_{1,1}$	$c_{1,1}$	$d_{1,1}$	$c_{2,0}$	$d_{2,0}$	$b_{0,2}$	$d_{0,2}$	$a_{2,1}$	$b_{2,1}$	$c_{2,1}$	$d_{2,1}$
$d_{0,0}$	1	0	0	$\frac{2\sqrt{2}}{\pi}$	$\frac{2\sqrt{2}}{\pi}$	0	0	0	0	0	0	$\frac{2\sqrt{2}}{\pi}$	0	0	0	0	0
$c_{1,0}$		1	0	0	0	$\frac{2\sqrt{2}}{\pi}$	0	$\frac{2\sqrt{2}}{\pi}$	0	0	0	0	0	0	0	0	0
$d_{1,0}$			1	0	0	0	$\frac{2\sqrt{2}}{\pi}$	0	$\frac{2\sqrt{2}}{\pi}$	0	0	0	0	0	0	0	0
$b_{0,1}$				1	$\frac{2}{\pi}$	0	0	0	0	0	0	$\frac{8}{3\pi}$	$\frac{-4}{3\pi}$	0	0	0	0
$d_{0,1}$					1	0	0	0	0	0	0	$\frac{8}{3\pi}$	$\frac{4}{3\pi}$	0	0	0	0
$a_{1,1}$						1	0	$\frac{2}{\pi}$	0	0	0	0	0	0	0	0	0
$b_{1,1}$							1	0	$\frac{2}{\pi}$	0	0	0	0	0	0	0	0
$c_{1,1}$								1	0	0	0	0	0	0	0	0	0
$d_{1,1}$									1	0	0	0	0	0	0	0	0
$c_{2,0}$										1	0	0	0	$\frac{2\sqrt{2}}{\pi}$	0	$\frac{2\sqrt{2}}{\pi}$	0
$d_{2,0}$											1	0	0	0	$\frac{2\sqrt{2}}{\pi}$	0	$\frac{2\sqrt{2}}{\pi}$
$b_{0,2}$												1	0	0	0	0	0
$d_{0,2}$													1	0	0	0	0
$a_{2,1}$														1	0	$\frac{2}{\pi}$	0
$b_{2,1}$															1	0	$\frac{2}{\pi}$
$c_{2,1}$																1	0
$d_{2,1}$																	1

Table 2. Effelsberg 100-m telescope horizontal pointing residuals (arcsec).

$A =$	10°	30	50	70	90	110	130	150	170	190	210	230	250	270	290	310	330	350
$a = 5°$																		
10				−9				−11										
15	−4			−6	+3			−9	−7			+1	+1	−1	+9	+9		−1
20	−1	−6		−5	+1	+4	+11	+8	−2	−1	−2	−5		+3	+5	+5	0	+2
25	0	−5		0		+3	0	+6	0	−1	−2	+6			+9		0	−3
30	−2	−5	+7	−5	+2	−1	+3		−2	0	−2		−1	+1	+7	+5	0	+1
35	−3	−5	−4	+2	+5	+1		+6	+3	0	−2	−1	0		+5	+8	−2	−2
40	−5	−5	−6	−2	+2	+2		+2	0		−2	−1	+2	0	+6	+2	−3	
45		−5	−6		+1	0	−1	−1		+1	−1	−1		−3		+2	−3	
50	−1	−4	−7	+4	+2	0		−2	−1	−1	0			0	+7	0	0	+2
55		−4	−3	−6		+5	−1		0	−2	0		−1	0	+6	0		
60	−3	−4	−4	−6	+1	+1	−2		0				0		0		−4	0
65		−2	−1	−1	+2		0					+1	−2		+3		−2	
70	+1	0	−3	−4		+4	0	−2		+3	−1		−3		+1			+3
75		−2	−2		+1		−1		+2	+1			0		+6		+1	
80	+1	0		−2			+3	+1	0	+1	−1						+5	+3
85																		